

## Raising the Spin-Reversal Barrier in Cyano-Bridged Single-Molecule Magnets: Linear $\text{Mn}^{\text{III}}_2\text{M}^{\text{III}}(\text{CN})_6$ ( $\text{M} = \text{Cr}, \text{Fe}$ ) Species Incorporating $[(5\text{-Brsalen})\text{Mn}]^+$ Units

Hye Jin Choi, Jennifer J. Sokol, and Jeffrey R. Long\*

Department of Chemistry, University of California, Berkeley, California 94720

Received November 17, 2003

Reactions between  $\text{K}_3[\text{M}(\text{CN})_6]$  and  $[\text{Mn}(5\text{-Brsalen})(\text{H}_2\text{O})_2]^+$  (5-Brsalen = *N,N'*-ethylenebis(5-bromosalicylidene)aminato dianion) in a mixture of methanol and water afford the compounds  $\text{K}[(5\text{-Brsalen})_2(\text{H}_2\text{O})_2\text{Mn}_2\text{M}(\text{CN})_6] \cdot 2\text{H}_2\text{O}$ , with  $\text{M} = \text{Cr}$  (**1**) or  $\text{Fe}$  (**2**). The two compounds are isostructural, each containing a molecular cluster with a linear  $\text{Mn}^{\text{III}}\text{—NC—M}^{\text{III}}\text{—CN—Mn}^{\text{III}}$  core and tetragonally elongated coordination about the  $\text{Mn}^{\text{III}}$  centers. Magnetic data indicate the presence of weak exchange interactions within the clusters, giving rise to ground states of  $S = 5/2$  and  $9/2$  with significant zero-field splitting. Despite the proximity of spin-excited states, ac susceptibility data reveal frequency-dependent out-of-phase signals characteristic of single-molecule magnets with spin-reversal barriers of  $U_{\text{eff}} = 16$  and  $25 \text{ cm}^{-1}$ , respectively.

Over a decade ago, it was discovered that the negative axial zero-field splitting parameter  $D$  associated with the  $S = 10$  ground state of  $[\text{Mn}_{12}\text{O}_{12}(\text{CH}_3\text{CO}_2)_{16}(\text{H}_2\text{O})_4]$  gives rise to slow paramagnetic relaxation.<sup>1</sup> The ensuing search for molecules with a larger spin-reversal barrier ( $U = S^2|D|$  or  $(S^2 - 1/4)|D|$  for integer and half-integer values of  $S$ , respectively) has since yielded a range of transition metal–oxo species exhibiting similar behavior.<sup>2</sup> The highest barrier observed for such a single-molecule magnet, however, is still just  $U_{\text{eff}} = 56 \text{ cm}^{-1}$ , occurring in the bromoacetate-substituted analogue of the original  $\text{Mn}_{12}\text{O}_{12}$  cluster.<sup>3</sup> Recently, many researchers have focused upon synthesizing metal–cyanide clusters, for which the parameters  $S$  and  $D$  are more readily

varied within a structure type via substitution of different transition metal ions.<sup>4,5</sup> Thus, for example, replacing the  $\text{Cr}^{\text{III}}$  centers in  $[(\text{Me}_3\text{tacn})_6\text{MnCr}_6(\text{CN})_{18}]^{2+}$  with  $\text{Mo}^{\text{III}}$  was shown to increase anisotropy, generating a barrier of  $U_{\text{eff}} = 10 \text{ cm}^{-1}$ .<sup>5c,e</sup> Surprisingly, few of the cyano-bridged molecules tested for this behavior have included  $\text{Mn}^{\text{III}}$  ions,<sup>4h,5f</sup> which provide the main source of anisotropy in the  $\text{Mn}_{12}\text{O}_{12}$  clusters. Herein, we report that linear  $\text{Mn}_2\text{M}(\text{CN})_6$  ( $\text{M} = \text{Cr}, \text{Fe}$ ) species incorporating Schiff base  $\text{Mn}^{\text{III}}$  complexes indeed behave as single-molecule magnets.

A tetragonal elongation in the octahedral coordination geometry of a high-spin  $\text{Mn}^{\text{III}}$  complex has long been known to result in a  $^5\text{B}_{1g}$  ground state with negative axial zero-field splitting.<sup>6</sup> For Schiff base complexes in particular, the magnitude of the distortion is comparable to that observed in  $[\text{Mn}_{12}\text{O}_{12}(\text{CH}_3\text{CO}_2)_{16}(\text{H}_2\text{O})_4]$ ,<sup>7</sup> and  $D$  values tend to fall within the range  $-1$  to  $-4 \text{ cm}^{-1}$ .<sup>8</sup> Such complexes have been shown to react with hexacyanometalate ions to produce a variety of cyano-bridged frameworks<sup>9</sup> and molecular clusters.<sup>5f,9a,c,10</sup> Among the latter species,  $[(5\text{-Brsalen})_2(\text{H}_2\text{O})_2\text{Mn}_2\text{Fe}(\text{CN})_6]^-$  caught our attention, owing to its proposed geometry in which the elongation axes for the two  $\text{Mn}^{\text{III}}$  centers are collinear.<sup>9a</sup> Moreover, the magnetic susceptibility

\* Author to whom correspondence should be addressed. E-mail: jlong@cchem.berkeley.edu.

- (1) (a) Sessoli, R.; Tsai, H.-L.; Schake, A. R.; Wang, J. B.; Folting, K.; Gatteschi, D.; Christou, G.; Hendrickson, D. N. *J. Am. Chem. Soc.* **1993**, *115*, 1804. (b) Sessoli, R.; Gatteschi, D.; Caneschi, A.; Novak, M. A. *Nature* **1993**, *365*, 141.
- (2) Selected references: (a) Barra, A.-L.; Debrunner, P.; Gatteschi, D.; Schulz, C. E.; Sessoli, R. *Europhys. Lett.* **1996**, *35*, 133. (b) Aubin, S. M. J.; Wemple, M. W.; Adams, D. M.; Tsai, H.-L.; Christou, G.; Hendrickson, D. N. *J. Am. Chem. Soc.* **1996**, *118*, 7746. (c) Castro, S. L.; Sun, Z.; Grant, C. M.; Bollinger, J. C.; Hendrickson, D. N.; Christou, G. *J. Am. Chem. Soc.* **1998**, *120*, 2365. (d) Barra, A. L.; Caneschi, A.; Cornia, A.; Fabrizi de Biani, F.; Gatteschi, D.; Sangregorio, C.; Sessoli, R.; Sorace, L. *J. Am. Chem. Soc.* **1999**, *121*, 5302. (e) Brechin, E. K.; Soler, M.; Davidson, J.; Hendrickson, D. N.; Parsons, S.; Christou, G. *Chem. Commun.* **2002**, 2252. (f) Murrie, M.; Teat, S. J.; Stoeckli-Evans, H.; Güdel, H. U. *Angew. Chem., Int. Ed.* **2003**, *42*, 4653.
- (3) Tsai, H.-L.; Chen, D.-M.; Yang, C.-I.; Jwo, T.-Y.; Wur, C.-S.; Lee, G.-H.; Wang, Y. *Inorg. Chem. Commun.* **2001**, *4*, 511.

- (4) Selected references: (a) Mallah, T.; Auberger, C.; Verdager, M.; Veillet, P. *J. Chem. Soc., Chem. Commun.* **1995**, 61. (b) Scullier, A.; Mallah, T.; Verdager, M.; Nivorzhkin, A.; Tholence, J.-L.; Veillet, P. *New J. Chem.* **1996**, *20*, 1. (c) Oshio, H.; Tamada, O.; Onodera, H.; Ito, T.; Ikoma, T.; Tero-Kubota, S. *Inorg. Chem.* **1999**, *38*, 5686. (d) Zhong, Z. J.; Seino, H.; Mizobe, Y.; Hidai, M.; Fujishima, A.; Ohkoashi, S.; Hashimoto, K. *J. Am. Chem. Soc.* **2000**, *122*, 2952. (e) Larionova, J.; Gross, M.; Andres, H.; Stoeckli-Evans, H.; Güdel, H. U.; Decurtins, S. *Angew. Chem., Int. Ed.* **2000**, *39*, 1605. (f) Parker, R. J.; Spiccia, L.; Berry, K. J.; Fallon, G. D.; Moubarak, B.; Murray, K. S. *Chem. Commun.* **2001**, 333. (g) Lescouezec, R.; Vaisserman, J.; Lloret, F.; Julve, M.; Verdager, M. *Inorg. Chem.* **2002**, *41*, 5943. (h) Berlingeutte, C. P.; Vaughn, D.; Cañada-Vilata, C.; Galán-Mascarós, J. R.; Dunbar, K. R. *Angew. Chem., Int. Ed.* **2003**, *42*, 1523. (i) Marvaud, V.; Decroix, C.; Scullier, A.; Guyard-Duhayon, C.; Vaisserman, J.; Gonnet, F.; Verdager, M. *Chem. Eur. J.* **2003**, *9*, 1678.
- (5) (a) Heinrich, J. L.; Berseth, P. A.; Long, J. R. *Chem. Commun.* **1998**, 1231. (b) Berseth, P. A.; Sokol, J. J.; Shores, M. P.; Heinrich, J. L.; Long, J. R. *J. Am. Chem. Soc.* **2000**, *122*, 9655. (c) Heinrich, J. L.; Sokol, J. J.; Hee, A. G.; Long, J. R. *J. Solid State Chem.* **2001**, *159*, 293. (d) Shores, M. P.; Sokol, J. J.; Long, J. R. *J. Am. Chem. Soc.* **2002**, *124*, 2279. (e) Sokol, J. J.; Hee, A. G.; Long, J. R. *J. Am. Chem. Soc.* **2002**, *124*, 7656. (f) Choi, H. J.; Sokol, J. J.; Long, J. R. *J. Phys. Chem. Solids*, in press.
- (6) Gritsen, H. J.; Sabisky, E. S. *Phys. Rev.* **1963**, *132*, 1507.
- (7) Lis, T. *Acta Crystallogr. B* **1980**, *36*, 2042.
- (8) Kennedy, B. J.; Murray, K. S. *Inorg. Chem.* **1985**, *24*, 1552.

data for this cluster were interpreted as indicating the presence of ferromagnetic exchange coupling and a negative axial zero-field splitting,<sup>9a</sup> making it a good candidate for a single-molecule magnet.

The cluster-containing compounds  $K[(5\text{-Brsalen})_2(\text{H}_2\text{O})_2\text{Mn}_2\text{M}(\text{CN})_6] \cdot 2\text{H}_2\text{O}$ , where  $\text{M} = \text{Cr}$  (**1**) and  $\text{Fe}$  (**2**), were synthesized by direct combination of their molecular components. A solution of  $\text{K}_3[\text{Cr}(\text{CN})_6]$  (41 mg, 0.13 mmol) in 1 mL of water was added to a solution of  $[\text{Mn}(5\text{-Brsalen})(\text{H}_2\text{O})_2]\text{ClO}_4$  (69 mg, 0.11 mmol) in 10 mL of methanol, and the mixture was stirred for 30 min to give a yellow-brown precipitate. The solid was collected by filtration, washed with 6 mL of a 1:1 mixture of methanol and water, and dried in air to give 51 mg (70%) of **1**.<sup>11</sup> An analogous procedure yielded 230 mg (73%) of **2**, also as a yellow-brown solid.<sup>12</sup> In each case, dark brown plate-shaped crystals suitable for X-ray analysis<sup>13</sup> were obtained simply by layering the solutions of the reactants.

Compounds **1** and **2** are isostructural, both containing a linear  $[(5\text{-Brsalen})_2(\text{H}_2\text{O})_2\text{Mn}_2\text{M}(\text{CN})_6]^-$  cluster in which an octahedral  $[\text{M}(\text{CN})_6]^{3-}$  complex is sandwiched between a pair of  $[\text{Mn}(5\text{-Brsalen})(\text{H}_2\text{O})_2]^+$  units. As shown for **1** in Figure 1, the  $\text{Mn}^{\text{III}}$  centers are bound through the nitrogen ends of trans cyanide groups, with a long  $\text{Mn}-\text{N}(1)$  separation of 2.342(4) Å and a significantly bent  $\text{Mn}-\text{N}(1)-\text{C}(1)$  angle of 141.8(4)°. The opposing coordination site on each  $\text{Mn}^{\text{III}}$  center is taken up by a water molecule, with a  $\text{Mn}-\text{O}(3)$  separation of 2.220(4) Å. As expected, these distances are significantly longer than those associated with the 5-Brsalen ligand, which binds with mean  $\text{Mn}-\text{N}$  and  $\text{Mn}-\text{O}$  distances of 1.985(2) and 1.886(2) Å, respectively. The resulting ratio of axial:equatorial ligand distances is 1.18, only slightly higher than the corresponding ratio of 1.13 in the structure of  $[\text{Mn}_{12}\text{O}_{12}(\text{CH}_3\text{CO}_2)_{16}(\text{H}_2\text{O})_4] \cdot 2\text{CH}_3\text{CO}_2\text{H} \cdot 4\text{H}_2\text{O}$ .<sup>7</sup> Although not perfectly collinear, the elongation axes associated with the two  $\text{Mn}^{\text{III}}$  centers in the cyano-bridged

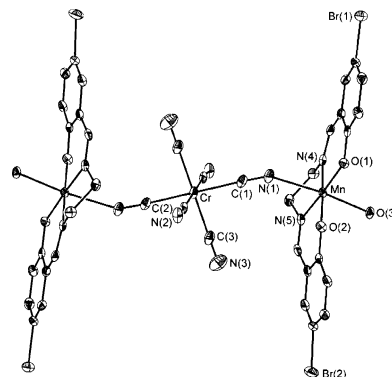


**Figure 1.** Structure of the linear  $[(5\text{-Brsalen})_2(\text{H}_2\text{O})_2\text{Mn}_2\text{Cr}(\text{CN})_6]^-$  cluster in **1**; H atoms are omitted for clarity. The molecule resides on an inversion center within the crystal. Selected interatomic distances (Å) and angles (deg): mean  $\text{Cr}-\text{C}$  2.071(2), mean  $\text{C}\equiv\text{N}$  1.155(3),  $\text{Mn}-\text{N}(4)$  1.981(3),  $\text{Mn}-\text{N}(5)$  1.988(3),  $\text{Mn}-\text{O}(1)$  1.873(3),  $\text{Mn}-\text{O}(2)$  1.898(3),  $\text{Mn}-\text{N}(1)$  2.342(4),  $\text{Mn}-\text{O}(3)$  2.220(4),  $\text{C}(1)-\text{Cr}-\text{C}(2)$  89.9(2),  $\text{C}(2)-\text{Cr}-\text{C}(3)$  92.9(2),  $\text{C}(1)-\text{Cr}-\text{C}(3)$  89.5(2),  $\text{Cr}-\text{C}(1)-\text{N}(1)$  176.9(4),  $\text{Cr}-\text{C}(2)-\text{N}(2)$  176.6(4),  $\text{Cr}-\text{C}(3)-\text{N}(3)$  176.6(4),  $\text{N}(1)-\text{Mn}-\text{N}(4)$  88.8(1),  $\text{N}(1)-\text{Mn}-\text{N}(5)$  85.2(1),  $\text{N}(4)-\text{Mn}-\text{O}(3)$  90.2(1),  $\text{N}(5)-\text{Mn}-\text{O}(3)$  86.4(1),  $\text{O}(1)-\text{Mn}-\text{N}(1)$  94.7(1),  $\text{O}(2)-\text{Mn}-\text{N}(1)$  91.5(1),  $\text{O}(1)-\text{Mn}-\text{O}(3)$  93.7(1),  $\text{O}(2)-\text{Mn}-\text{O}(3)$  88.7(1),  $\text{N}(1)-\text{Mn}-\text{O}(3)$  171.6(1),  $\text{Mn}-\text{C}(1)-\text{N}(1)$  141.8(4).

cluster are rigorously parallel by virtue of its crystallographic inversion symmetry. Note that the bromine substituents on the 5-Brsalen ligand appear to be essential for forming such trinuclear species, since related reactions employing the less sterically demanding salen ligand instead lead to the heptanuclear clusters  $[(\text{salen})_6(\text{H}_2\text{O})_6\text{Mn}_6\text{M}(\text{CN})_6]^{3+}$ .<sup>10</sup> While these larger molecules can have a higher-spin ground state, they do not necessarily exhibit the negative axial zero-field splitting parameter required of a single-molecule magnet, perhaps as a consequence of the conflicting orientations of the elongation axes about the  $\text{Mn}^{\text{III}}$  centers.<sup>5f</sup>

Dc magnetic susceptibility measurements were performed on **1** to probe the nature of the magnetic exchange coupling within the  $\text{Mn}_2\text{Cr}$  cluster. At 295 K, the compound exhibits  $\chi_{\text{M}}T = 6.480 \text{ cm}^3\text{K/mol}$ , which is somewhat below the spin-only value of  $7.878 \text{ cm}^3\text{K/mol}$  expected for one  $\text{Cr}^{\text{III}}$  ( $S = 3/2$ ) and two  $\text{Mn}^{\text{III}}$  ( $S = 2$ ) centers with  $g = 2.00$  and in the absence of any exchange coupling. With decreasing temperature,  $\chi_{\text{M}}T$  drops steadily to  $3.924 \text{ cm}^3\text{K/mol}$  at 40 K, and then more precipitously to  $1.255 \text{ cm}^3\text{K/mol}$  at 5 K (see Figure S1 in the Supporting Information). The initial trend indicates the presence of antiferromagnetic exchange coupling between the  $\text{Cr}^{\text{III}}$  and  $\text{Mn}^{\text{III}}$  centers, affording an  $S = 5/2$  ground state. Indeed, the data above 40 K were readily fit using MAGFIT 3.1<sup>14</sup> and an exchange Hamiltonian of the form  $\hat{H} = -2\hat{J}_{\text{Cr}} \cdot (\hat{S}_{\text{Mn}(1)} + \hat{S}_{\text{Mn}(2)})$  to give  $J = -6.3 \text{ cm}^{-1}$  and  $g = 1.912$ . This represents significantly stronger coupling than apparent in  $[(\text{salen})_6(\text{H}_2\text{O})_6\text{Mn}_6\text{Cr}(\text{CN})_6]^{3+}$ , for which  $J = -2.5 \text{ cm}^{-1}$ .<sup>5f</sup> A similar trend wherein  $J$  diminishes as the number of exchange pathways increases has been noted previously for cyano-bridged clusters.<sup>5d</sup> In accord with the field dependence of the magnetization data for **1** (see Figure S2, Supporting Information), the enhanced decay of  $\chi_{\text{M}}T$  at very low temperatures is attributed to zero-field splitting in the  $S = 5/2$  ground state of the  $\text{Mn}_2\text{Cr}$  cluster.

As shown in the upper panel of Figure 2, compound **2** exhibits substantially different magnetic behavior. At 295

- (9) (a) Miyasaka, H.; Matsumoto, N.; Okawa, H.; Re, N.; Gallo, E.; Floriani, C. *J. Am. Chem. Soc.* **1996**, *118*, 981. (b) Miyasaka, H.; Matsumoto, N.; Re, N.; Gallo, E.; Floriani, C. *Inorg. Chem.* **1997**, *36*, 670. (c) Miyasaka, H.; Ieda, H.; Matsumoto, N.; Re, N.; Crescenzi, R.; Floriani, C. *Inorg. Chem.* **1998**, *37*, 255. (d) Miyasaka, H.; Ieda, H.; Matsumoto, N.; Sugiura, K.-I.; Yamashita, M. *Inorg. Chem.* **2003**, *42*, 3509.
- (10) (a) Shen, X.; Li, B.; Zou, J.; Xu, Z. *Transition Met. Chem.* **2002**, *27*, 372. (b) Shen, X.; Li, B.; Zou, J.; Hu, H.; Xu, Z. *J. Mol. Struct.* **2003**, *657*, 325.
- (11) Characterization of **1**. IR (solid, ATR):  $\nu_{\text{CN}}$  2140, 2122  $\text{cm}^{-1}$ .  $\mu_{\text{eff}} = 7.16 \mu_{\text{B}}$  at 295 K. Anal. Calcd for  $\text{C}_{38}\text{H}_{32}\text{Br}_4\text{CrKMn}_2\text{N}_{10}\text{O}_8$ : C, 35.72; H, 2.53; N, 10.97. Found: C, 35.98; H, 2.52; N, 10.86. The X-ray powder diffraction pattern for this compound matches that simulated from its crystal structure.<sup>13</sup>
- (12) Characterization of **2**. IR (solid, ATR):  $\nu_{\text{CN}}$  2128, 2109 (sh), 2100  $\text{cm}^{-1}$ .  $\mu_{\text{eff}} = 6.95 \mu_{\text{B}}$  at 295 K. Anal. Calcd for  $\text{C}_{38}\text{H}_{32}\text{Br}_4\text{FeKMn}_2\text{N}_{10}\text{O}_8$ : C, 35.62; H, 2.52; N, 10.93. Found: C, 35.47; H, 2.46; N, 10.93. The X-ray powder diffraction pattern for this compound matches that simulated from its crystal structure.<sup>13</sup>
- (13) Crystal and structure refinement parameters: **1**,  $\text{C}_{38}\text{H}_{32}\text{Br}_4\text{CrKMn}_2\text{N}_{10}\text{O}_8$ ,  $T = 154 \text{ K}$ ,  $P2_1/c$ ,  $Z = 2$ ,  $a = 10.820(3) \text{ \AA}$ ,  $b = 14.054(4) \text{ \AA}$ ,  $c = 15.320(4) \text{ \AA}$ ,  $V = 2320.3(10) \text{ \AA}^3$ ,  $d_{\text{calc}} = 1.828 \text{ g/cm}^3$ ,  $R_1 = 0.0502$ ,  $wR_2 = 0.0998$ ; **2**,  $\text{C}_{38}\text{H}_{32}\text{Br}_4\text{FeKMn}_2\text{N}_{10}\text{O}_8$ ,  $T = 154 \text{ K}$ ,  $P2_1/c$ ,  $Z = 2$ ,  $a = 10.8285(18) \text{ \AA}$ ,  $b = 13.972(2) \text{ \AA}$ ,  $c = 15.154(3) \text{ \AA}$ ,  $V = 2282.7(7) \text{ \AA}^3$ ,  $d_{\text{calc}} = 1.852 \text{ g/cm}^3$ ,  $R_1 = 0.0529$ ,  $wR_2 = 0.0994$ . Data were collected using graphite monochromated Mo  $\text{K}\alpha$  radiation, and corrected for Lorentz, polarization, and absorption effects. The structures were refined against all data using SHELXTL 5.0.
- (14) Schmitt, E. A. Ph.D. Thesis, University of Illinois, 1995.

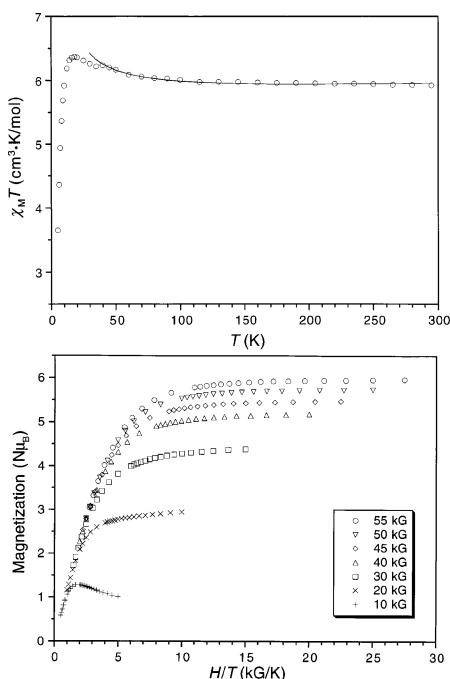


**Figure 2.** Magnetic behavior of **2**. Upper: Dc molar susceptibility data, as measured in an applied field of 10 kG. The solid line represents a calculated fit to the data; see text for details. Lower: Magnetization data in applied fields from 10 to 55 kG at temperatures between 2 and 20 K.

K,  $\chi_{MT}$  is  $5.927 \text{ cm}^3 \text{ K/mol}$ , only slightly less than the spin-only value of  $6.378 \text{ cm}^3 \text{ K/mol}$  expected for one  $\text{Fe}^{\text{III}}$  ( $S = 1/2$ ) ion and two  $\text{Mn}^{\text{III}}$  ( $S = 2$ ) ions with  $g = 2.00$  and in the absence of any exchange coupling. With decreasing temperature,  $\chi_{MT}$  gradually increases, achieving a maximum of  $6.372 \text{ cm}^3 \text{ K/mol}$  at 18 K before plummeting. The rise in  $\chi_{MT}$  indicates ferromagnetic coupling between the  $\text{Fe}^{\text{III}}$  and  $\text{Mn}^{\text{III}}$  centers, resulting in an  $S = 9/2$  ground state. Employing the same procedure as before, the data above 30 K were fit to give  $J = 2.3 \text{ cm}^{-1}$  and  $g = 1.900$ .<sup>15</sup> The coupling constant is in close agreement with the value of  $2J = 4.5 \text{ cm}^{-1}$  obtained for this compound previously by a different fitting method.<sup>9a</sup> The drop in  $\chi_{MT}$  at very low temperatures is again attributable to zero-field splitting.

Of the two clusters,  $[(5\text{-Brsalen})_2(\text{H}_2\text{O})_2\text{Mn}_2\text{Fe}(\text{CN})_6]^-$  has the higher spin ground state, and was therefore studied most intensively. The lower panel in Figure 2 shows the field dependence of the magnetization data for compound **2** at temperatures between 2 and 20 K. The nonsuperposition of the isofield lines clearly indicates the presence of significant zero-field splitting. Additionally, even at 55 kG and 2 K, the magnetization is still well below the saturation value of  $8.55 N\mu_B$  expected for an  $S = 9/2$  ground state with  $g = 1.900$  in the absence of zero-field splitting. Efforts to extract reliable zero-field splitting parameters from these data, however, were severely hampered by the presence of low-lying spin-excited states. Specifically, the very weak ferromagnetic exchange coupling within the cluster leads to  $S = 7/2$  and  $S = 5/2$  states located  $2.3$  and  $4.6 \text{ cm}^{-1}$  above the ground state, respectively. As a consequence, zero-field splittings on the order of  $1 \text{ cm}^{-1}$  in magnitude associated

(15) Note that this fit did not take the orbital degeneracy of the  $\text{Fe}^{\text{III}}$  center into account, and is therefore only approximate.

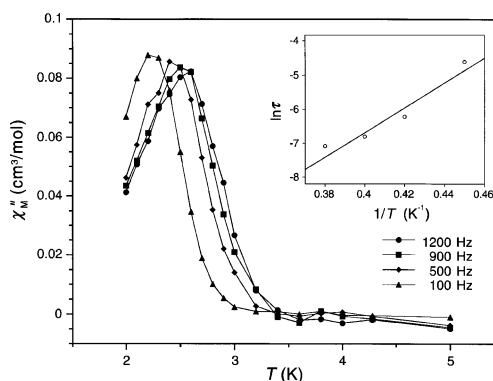


**Figure 3.** Out-of-phase component of the ac susceptibility for **2**, measured in a 1 G field oscillating at selected frequencies. The plot in the inset shows that the relaxation times,  $\tau$ , obtained from the peaks in the ac susceptibility conform to an Arrhenius relationship.

with any or all of these states results in mixing of the corresponding  $M_S$  levels. While reasonable simulations of the data could be obtained using three independent  $D$  values for these three lowest-energy spin states, the results are probably not reliable owing to overparametrization.

Despite the proximity of lower-spin excited states, ac magnetic susceptibility data collected on **2** in zero applied dc field manifest slow relaxation of the magnetization. As the frequency of the oscillating 1 G field increases, a lag in the in-phase component of the molar ac susceptibility,  $\chi_{M'}$ , is observed at low temperatures (see Figure S3, Supporting Information). The corresponding rise in the out-of-phase susceptibility,  $\chi_{M''}$  is shown in Figure 3 for switching frequencies of 100, 500, 900, and 1200 Hz. In each case,  $\chi_{M''}$  achieves a maximum at a temperature where it is assumed that the switching of the magnetic field matches the relaxation rate,  $1/\tau$ , for the magnetization of the cluster. As for other single-molecule magnets,<sup>1,2</sup> the ensuing relaxation times follow an Arrhenius relationship:  $\tau = \tau_0 \exp(U_{\text{eff}}/k_B T)$ . Accordingly, a plot of  $\ln \tau$  vs  $1/T$  is linear (see inset in Figure 3), with a least-squares fit yielding  $\tau_0 = 5.5 \times 10^{-10} \text{ s}$  and  $U_{\text{eff}} = 25 \text{ cm}^{-1}$ . Assuming that the slow relaxation stems exclusively from the  $S = 9/2$  ground state, the  $25 \text{ cm}^{-1}$  barrier sets a limit on the associated zero-field splitting parameter of  $D \leq -1.3 \text{ cm}^{-1}$ , which is very close to the value reported previously.<sup>9a</sup>

Interestingly, although the  $\text{Mn}_2\text{Cr}$  cluster possesses a ground state of just  $S = 5/2$ , it too behaves as a single-molecule magnet. A completely analogous interpretation of the ac susceptibility data for **1** (see Figures S4 and S5, Supporting Information) gave  $\tau_0 = 6.1 \times 10^{-8} \text{ s}$  and  $U_{\text{eff}} = 16 \text{ cm}^{-1}$ .

The foregoing results demonstrate the highest spin-reversal barriers yet observed for cyano-bridged single-molecule magnets. Efforts to incorporate Schiff base complexes of  $\text{Mn}^{\text{III}}$  into longer chain clusters with higher-spin ground states are underway.

**Acknowledgment.** This research was funded by NSF Grant CHE-0072691 and the Korean Science & Engineering Foundation (through a postdoctoral fellowship to H.J.C.). We thank Profs. J. K. McCusker and A. M. Stacy for use of the SQUID magnetometers.

**Supporting Information Available:** X-ray crystallographic files (CIF) and additional magnetic data for **1** and **2**. This material is available free of charge via the Internet at <http://pubs.acs.org>. IC035327Q